Inorganic Chemistry

ARTICLE

pubs.acs.org/IC

Hydrothermal Growth and Structural Studies of $Si_{1-x}Ge_xO_2$ Single Crystals

V. Ranieri,[†] S. Darracq,[‡] M. Cambon,[†] J. Haines,[†] O. Cambon,[*,†] A. Largeteau,[‡] and G. Demazeau[‡]

[†]Institut Charles Gerhardt Montpellier, UMR-CNRS-UM2-ENSCM-UM1 5253, Université Montpellier 2, Equipe C2M, Place E. Bataillon, 34095 Montpellier, Cedex 5, France

[‡]Institut de Chimie de la Matière Condensée de Bordeaux, CNRS, Université Bordeaux 1, site de l'ENSCPB, 87 avenue du Dr. A. Schweitzer, 33608 PESSAC Cedex, France

ABSTRACT: The substitution of germanium in the α-quartz structure is a method investigated to improve the piezoelectric properties and the thermal stability of α-quartz. Growth of α-quartz type $Si_{1-x}Ge_xO_2$ single crystals was performed using a temperature gradient hydrothermal method under different experimental conditions (pressure, temperature, nature of the solvent, and the nutrient). To avoid the difference of dissolution kinetics between pure SiO_2 and pure GeO_2, single phases $Si_{1-x}Ge_xO_2$ solid solutions were prepared and used as nutrients. The influence of the nature (cristobalite-type, glass) and the composition of this nutrient were also studied. Single crystals were grown in aqueous NaOH (0.2−1 M) solutions and in pure water. A wide range of pressures (95−280 MPa) and temperatures (315−505 °C) was investigated. Structures of single crystals with $x = 0.07$, 0.1, and 0.13 were refined, and it was shown that the structural distortion (i.e., θ and δ) increases with the atomic fraction of Ge in an almost linear way. Thus, the piezoelectric properties of $Si_{1-x}Ge_xO_2$ solid solution should increase with x, and this material could be a good candidate for technological applications requiring a high piezoelectric coupling factor or high thermal stability.

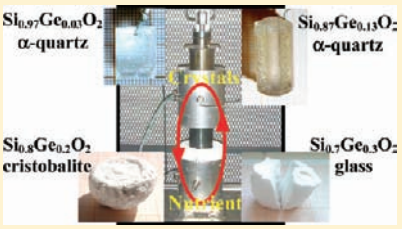

INTRODUCTION

Due to its piezoelectric properties, α-quartz is of great importance for the electronic industry. However, its physical properties are too limited for emerging applications that require a high thermal stability or a high electro-mechanical coupling coefficient. The structure of α-quartz homeotypes $Y^{IV}O_2$ (Y = Si, Ge) and $M^{III}X^{V}O_4$ (M^{III} = B, Al, Ga, Fe and X^{V} = P, As) belong to space groups $P3_121$ or $P3_221$ with $Z = 3$. The structure can be described as a helical chain of tetrahedra along the z axis. In these materials, structure−property relationships linking either the thermal stability of the α-quartz type phase or the physical properties (dielectric, piezoelectric...) to the structural distortion with respect to the β-quartz structure type have been developed.[1−8] This structural distortion can be described by the intertetrahedral bridging angle θ and the tetrahedral tilt angle δ, which is the order parameter for the $\alpha-\beta$ phase transition and corresponds to the rotation of the tetrahedra about their 2-fold axes parallel to x.[9] The distortion increases when θ increases and δ decreases. An almost linear dependence between the electromechanical coupling coefficient k and the structural distortion exists. The electromechanical coupling coefficient corresponds to the efficiency of the conversion between mechanical and electrical energy. In the quartz group, $GaAsO_4$[8] and GeO_2[7] have been found to be the most distorted. They have the highest coupling coefficients, and they do not undergo a ($\alpha-\beta$) phase transition. Several solid solutions have been studied among the α-quartz homeotypes: SiO_2-GeO_2,[10−16] SiO_2-PON,[4] SiO_2-AlPO_4,[17] $AlPO_4-GaPO_4$,[18−23] $AlPO_4-AlAsO_4$,[24] $AlPO_4-FePO_4$,[25] and $GaPO_4-FePO_4$.[26] In the $Al_{1-x}Ga_xO_4$ system, it was shown that the substitution of the larger cation Ga increases the structural distortion[22] and the covalent behavior of the chemical bonds.[24] These results open a way to tune the piezoelectric properties by adjusting the chemical composition of solid solutions. Moreover, the $\alpha-\beta$ phase transition temperature increases with x, and the $\alpha-\beta$ phase transition is not observed for Ga-rich compositions which undergo reconstructive transitions to β-cristobalite forms.

Thus, the substitution of Ge atoms in the SiO_2 α-quartz structure is believed to be a promising method to improve the piezoelectric properties and the thermal stability of this material. The first measurements of the piezoelectric coefficients on a $Si_{0.93}Ge_{0.07}O_2$ crystal confirm that they are a bit higher than those of α-quartz.[16] The phase diagram of the SiO_2-GeO_2 system indicates that α-quartz type solid solutions exist with a maximum of 31 atomic % of GeO_2 at about 700 °C and 70 MPa under hydrothermal conditions.[11] Hydrothermal growth of quartz crystals is performed in alkaline solutions such as NaOH (1 M) and Na_2CO_3 (0.8 M) at about 150 MPa and 360 °C. These conditions are not suitable to the growth of $Si_{1-x}Ge_xO_2$ crystals because of the formation of sodium germanates.[27−30] Experiments at higher pressures (up to 270 MPa)[17] and temperatures (up to 720 °C)[31] with dilute aqueous alkaline or fluoride solutions enable the Ge content to be increased, but these conditions are not appropriate for an industrial development. We report in this paper the development of a new growth process in order to optimize the Ge content in the $Si_{1-x}Ge_xO_2$ single crystals.

Received: February 18, 2011
Published: April 19, 2011

dx.doi.org/10.1021/ic200354p | *Inorg. Chem.* 2011, 50, 4632–4639

EXPERIMENTAL SECTION

1. Crystal Growth Apparatus. The growth of $Si_{1-x}Ge_xO_2$ single crystals with the α-quartz-type structure was performed using the temperature gradient hydrothermal method in 100 cm^3 and 300 cm^3 autoclaves made from Ni−Cr-based alloys. The internal volume was divided into two parts. Due to the direct solubility (S) of these materials (i.e., S increases with the temperature), the nutrient, which will be dissolved, was placed in a basket, in the bottom part of the autoclave at the highest temperature, and the seeds are fixed in the upper part at a lower temperature. The internal temperature was measured in both the nutrient dissolution and the crystal growth part of the autoclave with a multipoint J-type thermocouple linked to a Eurotherm regulator. The pressure was measured with an HBM pressure transducer (or sensor). The temperature range from 315 to 505 °C in the crystal growth part and pressure range from 99 to 280 MPa were investigated. The temperature gradient ranged from 7 to 35 °C. The influence of growth parameters and the solvent were studied and will be discussed.

2. Preparation of the Crystal Growth Experiments. Alkaline aqueous solutions of different concentrations from 0.2 to 1 M of NaOH and pure water were used as a solvent. Seeds, cut from synthetic α-quartz crystals in the shape of plates perpendicular to the z axis, were fixed in the upper part of the autoclave. The surfaces of the seeds were prepared by a chemical attack for three days in a 3 M sodium hydroxide solution at 70 °C.

3. Techniques of Crystal Characterization. The single crystals obtained were systematically cut in a direction perpendicular to the y axis (Y-cut), embedded in epoxy resin, polished optically, and then metalized in order to map the chemical composition using an electron probe microanalyzer (EPMA). Analysis was performed with a CAMECA SX-100 electron probe instrument equipped with five wavelength dispersive X-ray spectrometers (WDS).

Selected single crystal fragments were studied at 296 K by X-ray diffraction with an Oxford Diffraction Xcalibur 4-circle diffractometer equipped with a CCD detector using Mo Kα radiation (λ = 0.7107 Å). The intensity data were collected using the Crysalis CCD program. The cell parameters were refined, and the intensity data were indexed, reduced, and corrected for absorption using the Crysalis RED program.

The structure of $Si_{1-x}Ge_xO_2$ with x = 0.07, 0.1, and 0.13 was refined starting from an α-quartz-type structure model using SHELXL-97.[32]

RESULTS AND DISCUSSION

1. Nutrient Synthesis. The hydrothermal crystal growth is governed by a thermal cycle between the bottom (hot zone) and

Table 1. Synthesis Conditions of the $Si_{1-x}Ge_xO_2$ Nutrients

x_{Ge}	T_{max} (°C)	duration (h)	$T_{plateau}$ (°C)	duration (h)	phase	cooling
0.1	1685	46	1350	96	cristobalite	progressive
0.2	1685	24	1350	192	cristobalite	
0.25	1685	24	1350	240	glass	
0.3	1685	24	1400	96	glass	
0.3	1685	24	1350	168	glass	
0.4	1685	5	900	48	glass	
0.5	1685	10	1200	6 h	glass	
0.6	1450	6	1000	64	glass	quenched from 500 °C
0.7	1450	20	1000	86	glass	progressive in furnace
0.8	1685	10	1050	120	glass	quenched from 1050 °C

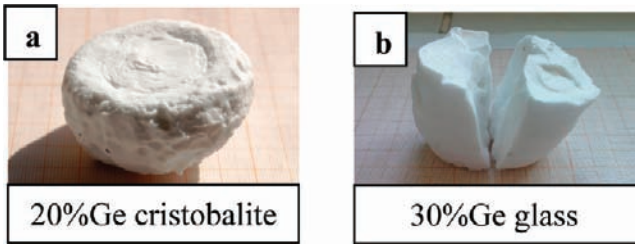

Figure 1. Photographs of $Si_{1-x}Ge_xO_2$ solid solutions used as nutrients (a) x = 0.2, cristobalite (b) x = 0.3, glass.

Table 2. Crystal Growth Experimental Parameters (C20 = Cristobalite-Type with 20 atom % Ge; G*xx* = Glass with *xx* atom % of Ge; ΔT = Thermal Gradient between the Dissolution and the Growth Part)

cycles	nutrient	$C_{solvent}$	P (MPa)	T_{growth} (°C)	ΔT (°C)	growth rate (mm/d)	$x_{average}$ (atom %)	duration (days)
Q1	C20	1 M	130	360	17	0.3	0	15
Q2	C20	0.5 M	207	315	15	0.23	1	18
Q3	C20	0.5 M	117	400	17	0.24	4.5	21
Q4	C20	0.5 M	107	495	22	0.27	2	20
Q5	G25	0.5 M	135	330	8	0.1	0	20
Q6	C20	0.5 M	122	340	15	0.18	1.9	22
Q7	C20	0.5 M	95	320	7	0.12	2.3	15
Q8	C20	0.4 M	150	445	15	0.15	3	27
Q9	G30	0.4 M	187	433	8			10
Q10	C20	0.3 M	125	505	15	1.2	5	12
Q11	G50	0.3M	136	340	20	0.08	3−6.5	38
Q12	G30	0.2 M	95	405	35			12
Q13	C20	0.2 M	144	423	17			24
Q14	C20	H_2O	250	410	20	0.16	6 −12	17
Q15	C20	H_2O	278	425	20	0.18	9−13	17
Q16	C20	H_2O	280	400	18	0.2	7.5	7
Q17	G30	H_2O	170	432	10	0.24	13− 23	11
Q18	G30	H_2O	175	415	10	0.23	5−14	25
Q19	G30	H_2O	99	440	20	0.15	8−16	12

dx.doi.org/10.1021/ic200354p |*Inorg. Chem.* 2011, 50, 4632–4639

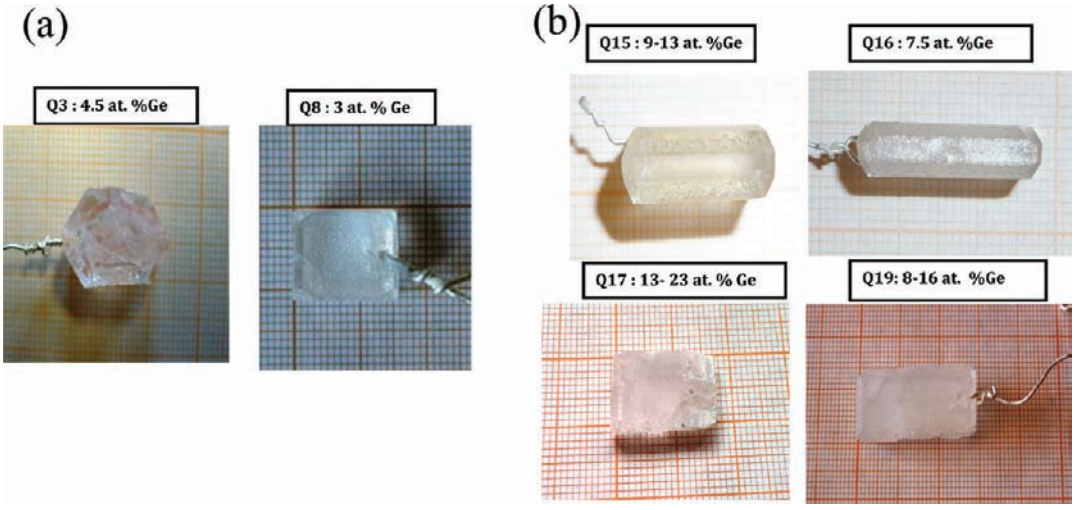

Figure 2. Photographs of crystals grown in (a) 0.5 M NaOH and (b) pure water.

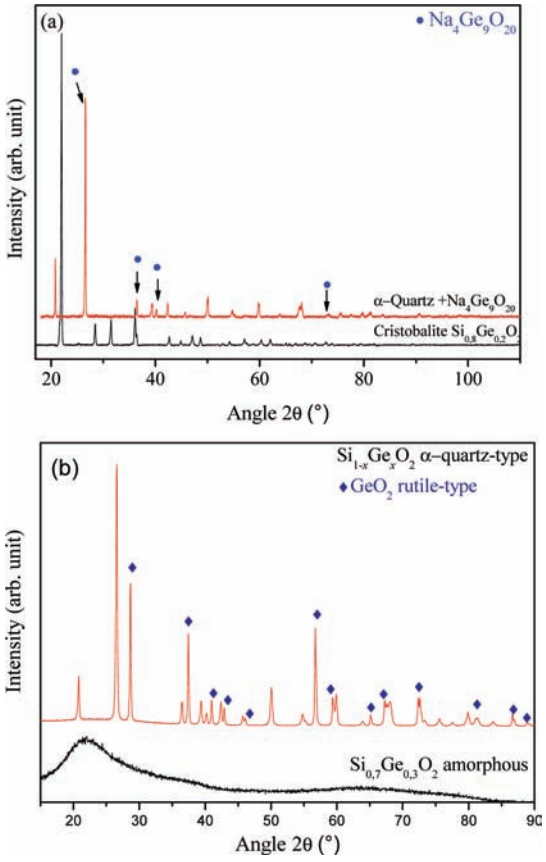

Figure 3. X-ray powder diffraction patterns of nutrient before and after growth experiments in (a) NaOH solution and (b) H_2O.

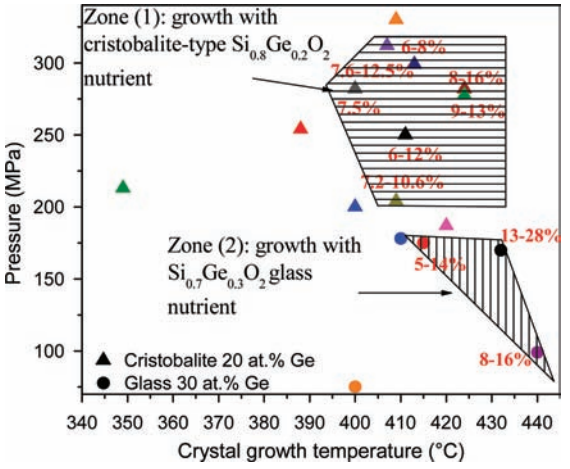

Figure 4. $P-T$ diagram of crystal growth experiments using pure water. Single crystals were obtained only in the hatched $P-T$ zone defined.

the upper part (cool zone) of the autoclave. The supersaturated conditions and the crystal growth rate (in the upper part) depend on the kinetics of the nutrient dissolution. To avoid the difference of the dissolution kinetics between the pure SiO_2 and GeO_2 compounds, $Si_{1-x}Ge_xO_2$ solid solutions, with $0.1 \leq x \leq 0.8$, were synthesized by thermal treatment in a Nabertherm HT04/17 type furnace and used as nutrients. Two types of materials were obtained as a function of the Ge atomic fraction: (i) a crystalline phase with the cristobalite-type structure for $x < 0.25$ and (ii) a glass for $x \geq 0.25$ (Table 1, Figure 1).

2. Crystal Growth Experiments. The crystal growth experiments parameters are given in Table 2, and photographs of selected crystals grown are presented in Figure 2.

a. NaOH Solvent. In the first experiments, diluted NaOH aqueous solutions were used in order to determine the influence of the alkaline concentration on the growth rate and the Ge content in the crystals. The growth rate decreases with the concentration of the solution, and below 0.2 M (Q13, Q12), no growth was observed. The temperature is the predominant parameter: as an exemple, the cycle Q10 ($T = 505$ °C) presents a growth rate 4 times higher than that of the cycle Q1 ($T = 360$ °C) despite the use of a less concentrated solution (0.3 and 1 M, respectively). The Ge content in the crystals remains low in all cycles using NaOH aqueous solution even for high temperature growth runs. Indeed, the substitution of Ge atoms is limited by the formation of sodium germanate $Na_4Ge_9O_{20}$. Germanium

dx.doi.org/10.1021/ic200354p |*Inorg. Chem.* 2011, 50, 4632–4639

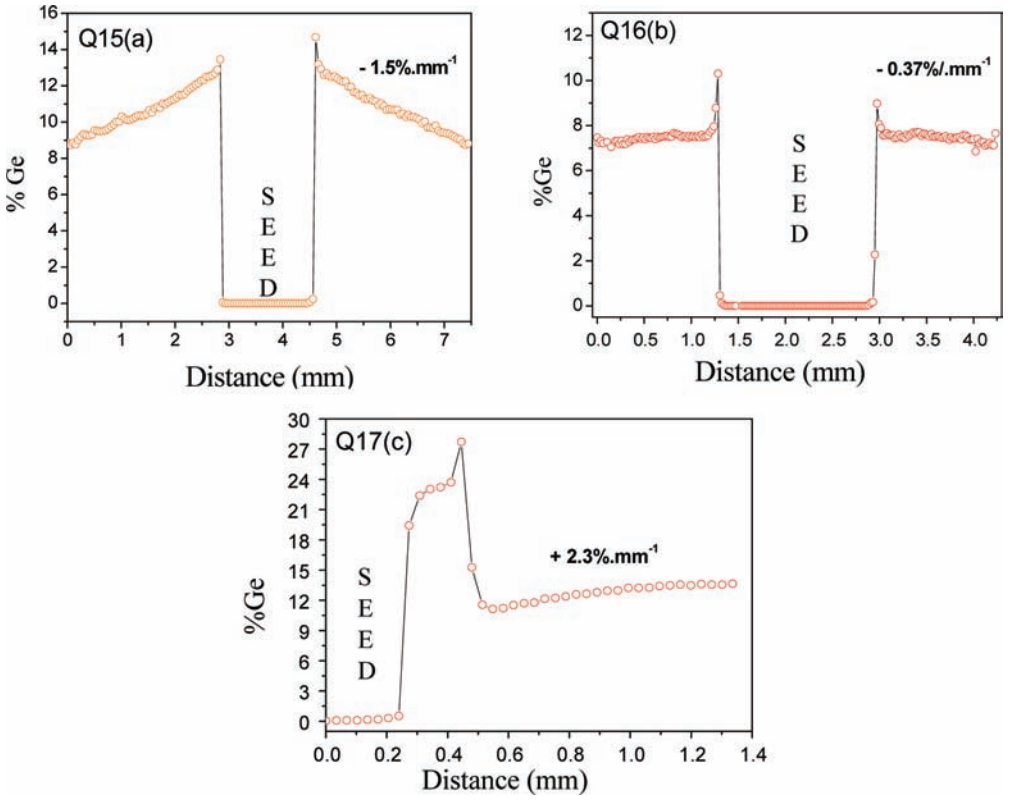

Figure 5. EPMA profiles of Ge concentration in crystals along the *z* axis. (a) Q15: $T = 425$ °C, $P = 278$ MPa. (b) Q16: $T = 400$ °C, $P = 280$ MPa. (c) Q17: $T = 432$ °C, $P = 170$ MPa.

trapped in the sodium germanate does not participate in the growth. These sodium germanates were identified by X-ray diffraction analysis of the nutrient after a growth cycle (Figure 3a). In addition, the solid solutions used as nutrients are metastable and transform to the less soluble stable phases (α-quartz and $Na_4Ge_9O_{20}$) during the cycles. Because of the slow dissolution kinetics of the stable phases, this phase transformation involves an important change of the growth rate. Thus, the values given in Table 2 are average values over the total duration of each cycle.

b. H_2O Solvent. In the second part of the experiments, the alkaline solution was replaced with pure water to avoid the formation of sodium germanates. In these runs, the thermodynamic parameters were modified in order to dissolve the nutrient and perform crystal growth. The results of the runs are summarized in Table 2 and in a $P-T$ diagram (Figure 4), where the resulting Ge content is given for each crystal. Two different domains are defined in this diagram corresponding to the experimental conditions of the two processes developed. The first domain (zone 1) contains the crystal growth performed from a cristobalite-type $Si_{0.8}Ge_{0.2}O_2$ nutrient. In this case, high pressures (>200 MPa) and high temperatures (>400 °C) are required for growth. All of the crystals grown contain a higher Ge content than those grown in aqueous NaOH solution, but the distribution of Ge is less homogeneous. The EPMA maps show an important decrease of the Ge content during growth along the *z* axis for most of the crystals grown (Figure 5). Crystals with less than 10 atomic % Ge obtained at a growth temperature lower than 415 °C are more homogeneous (Figure 5b). Temperature is an important parameter in Si/Ge substitution and has an effect on growth rate and especially on the Ge content. The Ge content increases with temperature, but it is not possible to grow crystals with the same stoichiometry as the nutrient, because of the high solubility of Ge. The second domain (zone 2) corresponds to crystal growth experiments performed using a $Si_{0.7}Ge_{0.3}O_2$ glass nutrient. This nutrient is more quickly soluble than the cristobalite-type nutrient; thus crystal growth can be performed at lower pressure, and the lifetime of the autoclave can be increased. The Ge content still changes during growth. However, it can be noted that for the cycle Q17 ($T = 432$ °C, $P = 170$ MPa), starting from the higher concentration near the seed, the Ge content decreases strongly and stabilizes at a lower value of around $x = 0.13$ (Figure 5c). This EPMA profile can be explained by the phase transformation of the nutrient. Indeed, like the previous experiments in NaOH aqueous solution, the X-ray powder diffraction of the nutrient after crystal growth indicates that the metastable nutrient transforms to stable phases, which are in this case a $Si_{1-x}Ge_xO_2$ α-quartz-type phase with less than 3 atom % Ge and a GeO_2 rutile-type phase. During the dissolution of the metastable nutrient, the Ge content increases quickly. Then, the nutrient transforms to stable phases, and so the solution becomes oversaturated with respect to these new phases. The Ge content decreases dramatically until it reaches an equilibrium state between dissolution and crystallization. The crystals with the higher content of Ge exhibit some cracks. There is a high degree of stress due to the difference in cell parameters between quartz seed and growth section accumulated at the seed/growth interface. This stress was released on cooling and generates cracks upon rapid cooling.

These experiments show that aqueous sodium hydroxide solutions are not suitable for the growth of mixed $Si_{1-x}Ge_xO_2$ single crystals even using a diluted NaOH aqueous solution and a

dx.doi.org/10.1021/ic200354p |*Inorg. Chem.* 2011, 50, 4632–4639

Table 3. Experimental Data—Single Crystal X-Ray Diffraction

	$Si_{0.93}Ge_{0.07}O_2$	$Si_{0.9}Ge_{0.1}O_2$	$Si_{0.87}Ge_{0.13}O_2$
temperature (K)	293(2)	293(2)	293(2)
space group	$P3_221$	$P3_221$	$P3_221$
a (Å)	4.9200 (2)	4.9201 (2)	4.9222 (2)
c (Å)	5.4195 (2)	5.4259 (3)	5.4247 (2)
V (Å^3)	113.61 (1)	113.751 (9)	113.825 (6)
density (g cm^{-3})	2.77	2.83	2.88
diffractometer	Oxford Instruments Xcalibur		
radiation type	Mo Kα		
wavelength	0.7107		
absorption correction	numerical		
μ (mm^{-1})	2.297	2.854	3.411
range of h, k, l	$-7 \le h \le 7$	$-7 \le h \le 7$	$-7 \le h \le 7$
	$-7 \le k \le 7$	$-7 \le k \le 7$	$-7 \le k \le 7$
	$-8 \le l \le 8$	$-8 \le l \le 8$	$-8 \le l \le 8$
no. of measured reflns	3932	3761	3785
no. of unique reflns	322	321	323
no. of observed reflns ($I > 2\sigma$)	311	299	319
$R_{equivalents}$	0.0228	0.0397	0.0189
R_{sigma}	0.0107	0.0194	0.0069
		Refinement	
extinction coef.	0.16(2)	0.37(3)	0.19(2)
R ($F_{obs} > 4\sigma$)	0.0122	0.0160	0.0106
Rw	0.0383	0.0355	0.0339
χ^2	1.274	1.135	1.421
no. of params	16	16	16
weighting scheme	$w = (\sigma^2F_o^2 + (0.0203P)^2 + 0.01P)^{-1}$	$w = (\sigma^2F_o^2 + (0.0168P)^2 + 0.0149P)^{-1}$	$w = (\sigma^2F_o^2 + (0.0138P)^2 + 0.0236P)^{-1}$
	$P = (F_o^2 + 2F_c)/3$	$P = (F_o^2 + 2F_c)/3$	$P = (F_o^2 + 2F_c)/3$

single phase nutrient. The formation of the sodium germanate limits the amount of germanium in the solid solution. This compound is stable in the pressure−temperature range, and the average Ge content does not exceed 5 atom % in the crystals. According to previous work,[17] it appears that at both high temperatures (>400 °C) and high pressures (>250 MPa) sodium germanate is no longer stable, and thus Ge is not trapped. However, these conditions strongly decrease the lifetime of the autoclave. Using pure water, all of the germanium contained in the nutrient can participate in the crystal growth process, and the variation of composition between the nutrient and the grown single crystal is only due to the difference in the solubility and transport rate of the solvated species. The transport of species is governed by the temperature gradient. A small gradient allows the difference of transport rate between the solvated species to be reduced and increases the crystal quality; however, it decreases the growth rate. A gradient of 10 °C seems to be a good compromise. The Ge content increases with the temperature, in contrast with the first experiments using sodium hydroxide, for which the temperature only has an effect on the growth rate. At high temperatures (>400 °C), the cooling rate at the end of the run has to be very slow (max. 7 °C/h) in order to avoid cracks. The use of water requires an increase of the pressure and the temperature in order to dissolve the nutrient. However, as a function of the nature of the mixed $Si_{1-x}Ge_xO_2$ nutrient (structure and composition), crystal growth can be performed at pressures below 200 MPa with a growth rate appropriate for industrial development (about 0.24 mm/day). At the present time, the use of pure water and a $Si_{0.7}Ge_{0.3}O_2$ glass nutrient at high temperatures and moderate pressures is promising. The effect of the thermal gradient on the crystal composition has to be studied precisely in order to improve the homogeneity of the crystals.

Table 4. Fractional Atomic Coordinates and Equivalent Isotropic Displacement Parameters (Å^2) for α-Quartz-Type $Si_{1-x}Ge_xO_2$

x	x (Si/Ge)	$100U_{eq}$	x_O	y_O	z_O	$100U_{eq}$
0.07	−0.4675 (1)	0.76 (1)	−0.4123 (2)	−0.2699 (2)	0.7833 (1)	1.41 (2)
0.10	0.46667 (8)	0.81 (1)	0.4123 (2)	0.2714 (2)	0.7821 (1)	1.56 (2)
0.13	−0.46607 (7)	0.77 (1)	−0.4117 (2)	−0.2724 (2)	0.7813 (1)	1.50 (2)

3. Structural Distortion: Single Crystal X-Ray Diffraction. High-quality single-crystal fragments with linear dimensions on the order of 200 μm were obtained for $x = 0.07$, 0.1, and 0.13. The $R_{equivalents}$, R_{sigma}, and agreement factors of the structural refinement indicate that the three samples studied have an excellent crystalline quality and present few defects. The growth processes developed are thus suitable to obtain high-quality crystals. Crystal quality is a fundamental parameter needed to design performing devices. The fractional atomic coordinates of $Si_{1-x}Ge_xO_2$ (x = 0.07, 0.1, 0.13) solid solutions (Tables 3−8) are found to vary continuously as a function of the composition for the range of composition studied. The bond distances and angles lie between the values observed for the pure end members,

dx.doi.org/10.1021/ic200354p |Inorg. Chem. 2011, 50, 4632–4639

Table 5. Anisotropic Atomic Displacement Parameters (Å^2) for α-Quartz-Type $Si_{1-x}Ge_xO_2$

	$100U_{11}$	$100U_{22}$	$100U_{33}$	$100U_{23}$	$100U_{13}$	$100U_{12}$
			$Si_{0.93}Ge_{0.07}O_2$			
Si/Ge	0.83 (1)	0.67 (2)	0.73 (2)	0.04 (1)	0.022 (6)	0.333 (8)
O	1.73 (4)	1.38 (4)	1.34 (4)	0.51 (3)	0.26 (3)	0.94 (3)
			$Si_{0.9}Ge_{0.1}O_2$			
Si/Ge	0.88 (2)	0.75 (2)	0.76 (2)	−0.04 (1)	−0.018 (7)	0.375 (9)
O	1.84 (5)	1.55 (4)	1.45 (4)	−0.56 (3)	−0.22 (4)	0.97 (4)
			$Si_{0.87}Ge_{0.13}O_2$			
Si/Ge	0.85 (1)	0.69 (1)	0.70 (1)	0.05 (1)	0.026 (5)	0.35 (1)
O	1.81 (4)	1.44 (3)	1.46 (3)	0.57 (3)	0.24 (3)	0.96 (3)

Table 6. Bond Distances (Å) for α-Quartz-Type $Si_{1-x}Ge_xO_2$[a]

x	(Si.Ge)−O_1	(Si.Ge)−O_2
0	*1.605*	*1.614*
0.07	1.612 (1)	1.623 (1)
0.1	1.614 (1)	1.627 (1)
0.13	1.617 (1)	1.629 (1)
1	*1.734*	*1.740*

[a] Corresponding values for α-quartz[34] and α-quartz-type GeO_2[7] are given in italics.

Table 7. Tetrahedral Bond Angles (deg) in α-Quartz-Type $Si_{1-x}Ge_xO_2$[a]

x	O_1−(Si.Ge)−O_2	O_2−(Si.Ge)−O_4	O_2−(Si.Ge)−O_3	O_1−(Si.Ge)−O_4
0	*110.5*	*108.8*	*108.9*	*109.3*
0.07	110.71 (5)	108.65 (2)	109.03 (7)	109.10 (6)
0.1	110.70 (6)	108.54 (2)	109.20 (7)	109.16 (8)
0.13	110.77 (5)	108.55 (2)	109.10 (7)	109.11 (6)
1	*113.0*	*106.3*	*107.8*	*110.4*

[a] Corresponding values for α-quartz and α-quartz-type GeO_2 are given in italics.

Table 8. Intertetrahedral Bridging and Tilt Angles (deg) in α-Quartz-Type $Si_{1-x}Ge_xO_2$[a]

x	(Si.Ge)−O−(Si.Ge)	δ
0	*143.6*	*16.2*
0.07	142.69 (6)	17.16 (4)
0.1	142.29 (7)	17.56 (4)
0.13	141.88 (6)	17.83 (4)
1	*130.05*	*26.6*

[a] Corresponding values for α-quartz and α-quartz-type GeO_2 are given in italics.

SiO_2 and GeO_2. This can be observed in the increase of the A−O bond lengths due to the larger size of Ge and internal distortion of the tetrahedra (Tables 7 and 8). The structure distorts in order to pack the larger GeO_4 tetrahedra with a small volume change. The crystal structure is given in Figure 6 for x = 0.13. The structural distortion (i.e., θ and δ) increases with the Ge substitution on the 3a site (Figures 7 and 8) and varies in an almost linear trend with the composition.

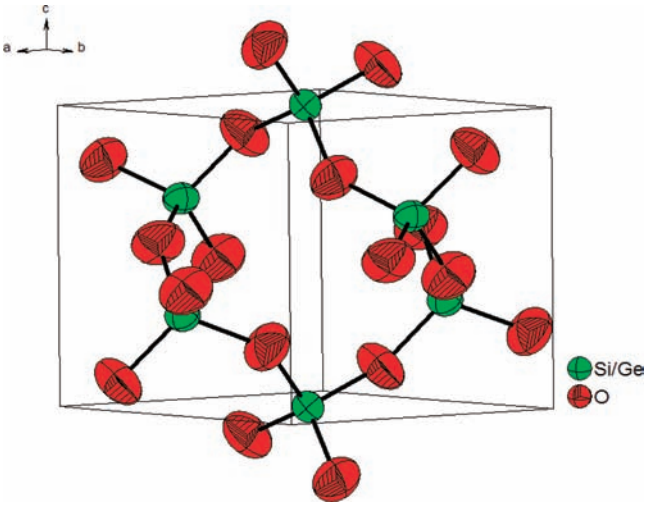

Figure 6. Crystal structure of $Si_{0.87}Ge_{0.13}O_2$ at 293 K. The ellipsoids are represented at 99% probability.

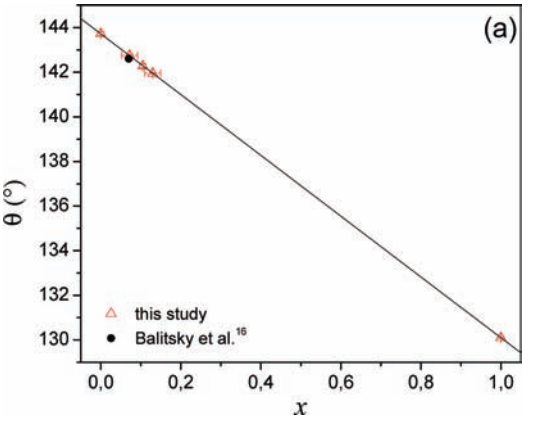

Figure 7. Plot of the intertetrahedral bridging angles in $Si_{1-x}Ge_xO_2$ crystals as a function of the composition.

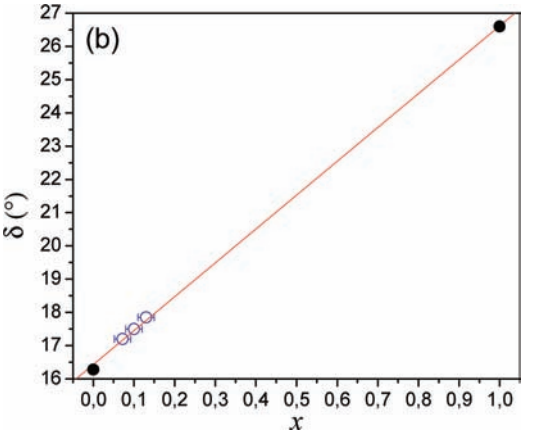

Figure 8. Plot of the tetrahedral tilt angles in $Si_{1-x}Ge_xO_2$ crystals as a function of the composition.

dx.doi.org/10.1021/ic200354p |*Inorg. Chem.* 2011, 50, 4632–4639

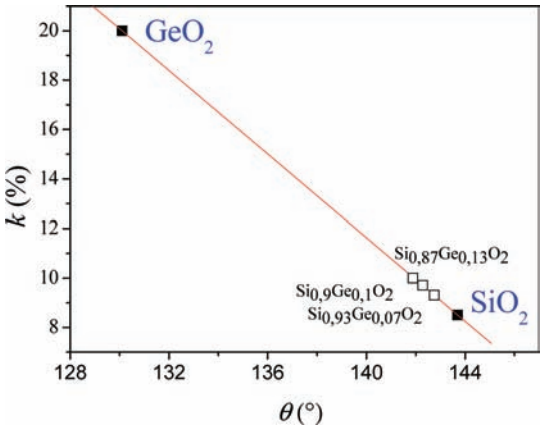

Figure 9. Plot of the piezoelectric coupling coefficient as a function of the intertetrahedral bridging angle. Open symbols represent the predicted values for $Si_{1-x}Ge_xO_2$ crystals.

The thermal stability of the α-quartz-type phase increases with the composition;[33] the transition to the β-phase occurs at 846 K for $x = 0$ and 1300 ± 50 K for $x = 0.24$. The elastic constants slightly decrease[16] with the Ge substitution, and thus the piezoelectric coupling coefficient can be expected to also vary as a function of composition (Figure 9). The ability to distort the structure with the substitution of a larger cation in these materials opens the possibility to tune their physical, thermodynamic, dielectric, and piezoelectric properties and thus design materials with optimal properties for a specific application.

CONCLUSION

Single crystals of formula $Si_{1-x}Ge_xO_2$ were grown using the hydrothermal method. The conventional conditions for the crystal growth of SiO_2 α-quartz using sodium hydroxide are not suitable for the growth of crystals belong to the solid solution. Two new processes were developed with pure water, a high pressure (>200 MPa), high-temperature (>400 °C) process using $Si_{0.8}Ge_{0.2}O_2$ cristobalite-type as a nutrient and a low-pressure (<200 MPa), high-temperature (>400 °C) process using $Si_{0.7}Ge_{0.3}O_2$ glass. The latter allows the Ge content in the crystals to be increased and to use thermodynamics parameters suitable for industrial development. It is found that the use of a mixed material as nutrient is very interesting for controlling the dissolution and as a consequence crystal growth. The Ge content in the crystals is highly dependent on the temperature in the growth part of the autoclave. High-quality single crystal samples with $x = 0.07$, 0.1, and 0.13 were studied using single-crystal X-ray diffraction. Final R factors of 1.32, 1.97, and 1.04% were obtained, respectively. The structural distortion is found to increase quite linearly with Ge substitution. According to structure−property relationships, an important improvement of the piezoelectric properties as a function of the composition can be expected for these materials. Thus, physical properties of the materials can be tuned by adjusting the chemical composition for a specific application.

AUTHOR INFORMATION

Corresponding Author

*E-mail: ocambon@lpmc.univ-montp2.fr.

ACKNOWLEDGMENT

The authors acknowledge C. Nevado (Atelier de Lithopréparation de L'ISTEEM, Université Montpellier 2), C. Merlet (Service Microsonde Sud, Université Montpellier 2), and D. Granier (Institut Gerhardt, Université Montpellier 2) for assistance with the sample preparation and data collection. The authors also thank the French Ministry of Defense for financial support (Contract No. 05 34 051).

REFERENCES

(1) Philippot, E.; Goiffon, A.; Ibanez, A.; Pintard, M. *J. Solid State Chem.* **1994**, *110*, 356.
(2) Philippot, E.; Palmier, D.; Pintard, M.; Goiffon, A. *J. Solid State Chem.* **1996**, *123*, 1–13.
(3) Philippot, E.; Armand, P.; Yot, P.; Cambon, O.; Goiffon, A.; Mcintyre, J.; Bordet, P. *J. Solid State Chem.* **1999**, *146*, 114–123.
(4) Haines, J.; Chateau, C.; Léger, J.-M.; Marchand, R. *Ann. Chim. Sci. Mater.* **2001**, *26*, 209–216.
(5) Haines, J.; Cambon, O.; Hull, S. *Z. Kristallogr.* **2003**, *218* (3), 193–200.
(6) Cambon, O.; Yot, P.; Ruhl, S.; Haines, J.; Philippot, E. *Solid State Sci.* **2003**, *5*, 469.
(7) Haines, J; Cambon, O; Philippot, E; Chapon, L; Hull, S *J. Solid State Chem.* **2002**, *166*, 434.
(8) Cambon, O.; Haines, J.; Fraysse, G.; Detaint, J.; Capelle, B.; Van der Lee, A. *J. Appl. Phys.* **2005**, 97.
(9) Grimm, H.; Dorner, B. *J. Phys. Chem. Solids* **1975**, *36*, 413.
(10) Miller, W. S.; Dachille, F.; Shafer, E. C.; Roy, R. *Am. Mineral.* **1963**, *48*, 1024.
(11) Shafer, E. C.; Shafer, M. W.; Roy, R. *Z. Kristallogr.* **1956**, 107.
(12) Fursenko, B. A.; Kirkinsky, V. A Rjaposov, A. P. *High-Pressure Proceeding Science and Technology-Proc.* 7th AIRAPT 1980, Int. Conf.; Vodar, B., Marteau, P., Eds.; Pergamon: Oxford, 1980; p 562.
(13) Balitsky, V. S.; Balitsky, D. V.; Nekrasov, A. N.; Balitskaya, L. V. *J. Phys. IV France* **2005**, *126*, 17–21.
(14) Largeteau, A.; Darracq, S.; Goglio, G. *Z. Naturforsch.* **2008**, *63b*, 739–741.
(15) Miclau, M.; Miclau, N.; Poienar, M.; Grozescu, I. *Cryst. Res. Technol.* **2009**, *44* (6), 577–580.
(16) Balitsky, V.; Detaint, J.; Armand, P.; Papet, P.; Balitsky, D. *Proceeding of the Frequency Control Symposium, Joint with the 21st EFTF Forum*; IEEE International: New York, 2007; pp 704−710.
(17) Veskler, I. V.; Thomas, R.; Wirth, R. *Am. Mineral.* **2003**, *88*, 1724.
(18) Cachau-Herreillat, D.; Bennazha, J.; Goiffon, A.; Ibanez, A.; Philippot, E. *Eur. J. Solid State Inorg. Chem.* **1992**, *29*, 1295.
(19) Xia, H. R.; Qin, Z. K.; Yuan, W.; Liu, S. F.; Zou, Z. Q.; Han, J. R. *Cryst. Res. Technol.* **1997**, *32*, 783.
(20) Xia, H.; Wang, J.; Li, L.; Zou, Z. *Prog. Cryst. Growth Char. Mater.* **2000**, *40*, 253.
(21) Haines, J.; Cambon, O.; Cachau-Herreillat, D.; Fraysse, G.; Mallassagne, F. E. *Solid States Sci.* **2004**, *6*, 995.
(22) Haines, J.; Cambon, O.; Fraysse, G.; Van der Lee, A. *J. Phys.: Condens. Matter* **2005**, *17*, 4463.
(23) Cambon, O.; Haines, J.; Cambon, M.; Keen, D. A.; Tucker, M. G.; Chapon, L.; Hansen, N. K.; Souhassou, M.; Porcher, F. *Chem. Mater.* **2009**, 237–246.
(24) Cachau-Herreillat, D.; Bennazha, J.; Goiffon, A.; Ibanez, A.; Philippot, E. *Eur. J. Solid State Inorg. Chem* **1992**, *29*, 1295.
(25) Mohamed, F. Sh. *Absorpt. Sci. Tech.* **2002**, *20*, 741.
(26) Miclau, M.; Bucur, R.; Vlazan, P.; Miclau, N.; Trusca, R.; Grozescu, I. *J. Opt. Adv. Mater.* **2007**, *9*, 2792–2794.
(27) Roy, R.; Theokritoff, S. *J. Cryst. Growth* **1972**, *12*, 69–72.
(28) Passaret, M.; Toudic, Y.; Regreny, A.; Aumont, R.; Bayon, J. F. *J. Cryst. Growth* **1972**, *13/14*, 524–529.

(29) Balitsky, D. V.; Balitsky, V. S.; Pushcharovsky, D. Yu; Bondarenko, G. V.; Kosenko, A. V. *J. Cryst. Growth* **1997**, *180*, 212–219.
(30) Balitsky, D. V.; Balitsky, V. S.; Pisarevsky, Y. V.; Philippot, E.; Silvestrova, O. Y.; Puscharovsky, D. Y. *Ann. Chim. Sci. Mater.* **2001**, *26* (1), 183–192.
(31) Balitsky, V. S.; Balitsky, D. V.; Nekrasov, A. N.; Balitskaya, L. V. *J. Cryst. Growth* **2005**, *275*, e807–e811.
(32) Sheldrick, G. M. *Acta Crystallogr.* **2009**, *A64*, 112–122.
(33) Ranieri, V.; Bourgogne, D.; Darracq, S.; Cambon, M.; Haines, J.; Cambon, O.; Le Parc, R.; Levelut, C.; Largeteau, A.; Demazeau, G. *Phys. Rev. B* **2009**, *79*, 224304.
(34) Kihara, K. *Eur. J. Mineral.* **1990**, *2*, 63–77.